



# Chromogranin A Promotes Peptide Hormone Sorting to Mobile Granules in Constitutively and Regulated Secreting Cells

Maite Montero-Hadjadje, Salah Elias, Laurence Chevalier, Magalie Benard, Yannick Tanguy, Valérie Turquier, Ludovic Galas, Laurent Yon, Maria M Malagon, Azeddine A. Driouich, et al.

## ► To cite this version:

Maite Montero-Hadjadje, Salah Elias, Laurence Chevalier, Magalie Benard, Yannick Tanguy, et al.. Chromogranin A Promotes Peptide Hormone Sorting to Mobile Granules in Constitutively and Regulated Secreting Cells. *Journal of Biological Chemistry*, 2009, 284 (18), pp.12420 - 12431. 10.1074/jbc.M805607200 . hal-01706423

HAL Id: hal-01706423

<https://normandie-univ.hal.science/hal-01706423>

Submitted on 19 Jul 2018

**HAL** is a multi-disciplinary open access archive for the deposit and dissemination of scientific research documents, whether they are published or not. The documents may come from teaching and research institutions in France or abroad, or from public or private research centers.

L'archive ouverte pluridisciplinaire **HAL**, est destinée au dépôt et à la diffusion de documents scientifiques de niveau recherche, publiés ou non, émanant des établissements d'enseignement et de recherche français ou étrangers, des laboratoires publics ou privés.



The Journal of  
Biological Chemistry

## AFFINITY SITES

ASBMB

American Society for Biochemistry and Molecular Biology

Molecular Basis of Cell and  
Developmental Biology:

### Chromogranin A Promotes Peptide Hormone Sorting to Mobile Granules in Constitutively and Regulated Secretory Cells: ROLE OF CONSERVED N- AND C-TERMINAL PEPTIDES

Maité Montero-Hadjadje, Salah Elias,  
Laurence Chevalier, Magalie Benard, Yannick  
Tanguy, Valérie Turquier, Ludovic Galas,  
Laurent Yon, Maria M. Malagon, Azeddine  
Driouich, Stéphane Gasman and Youssef  
Anouar

*J. Biol. Chem.* 2009, 284:12420-12431.

doi: 10.1074/jbc.M805607200 originally published online January 29, 2009

---

Access the most updated version of this article at doi: [10.1074/jbc.M805607200](https://doi.org/10.1074/jbc.M805607200)

Find articles, minireviews, Reflections and Classics on similar topics on the [JBC Affinity Sites](#).

#### Alerts:

- [When this article is cited](#)
- [When a correction for this article is posted](#)

[Click here](#) to choose from all of JBC's e-mail alerts

#### Supplemental material:

<http://www.jbc.org/content/suppl/2009/02/18/M805607200.DC1.html>

This article cites 45 references, 27 of which can be accessed free at  
<http://www.jbc.org/content/284/18/12420.full.html#ref-list-1>

# Chromogranin A Promotes Peptide Hormone Sorting to Mobile Granules in Constitutively and Regulated Secreting Cells

## ROLE OF CONSERVED N- AND C-TERMINAL PEPTIDES\*

Received for publication, July 22, 2008, and in revised form, January 21, 2009. Published, JBC Papers in Press, January 29, 2009, DOI 10.1074/jbc.M805607200

Maité Montero-Hadjadje<sup>†1</sup>, Salah Elias<sup>†1</sup>, Laurence Chevalier<sup>§</sup>, Magalie Benard<sup>¶1</sup>, Yannick Tanguy<sup>†</sup>, Valérie Turquier<sup>†</sup>, Ludovic Galas<sup>¶1</sup>, Laurent Yon<sup>†</sup>, Maria M. Malagon<sup>||</sup>, Azeddine Driouich<sup>§</sup>, Stéphane Gasman<sup>\*\*</sup>, and Youssef Anouar<sup>‡2</sup>

From <sup>†</sup>Équipe Associée 4310 *Neuronal and Neuroendocrine Differentiation and Communication*, INSERM U413, European Institute for Peptide Research (IFRMP 23), <sup>§</sup>Formation de Recherche en Evolution 3090 CNRS, IFRMP23, and the <sup>¶</sup>Platform for Cell Imaging of Normandy, IFRMP23, University of Rouen, 76821 Mont-Saint-Aignan, France, the <sup>||</sup>Department of Cell Biology, Physiology and Immunology, University of Cordoba, 14014 Cordoba, Spain, and the <sup>\*\*</sup>Department of Neurotransmission and Neuroendocrine Secretion, Unité Propre de Recherche 3212 CNRS, Institut des Neurosciences Cellulaires et Intégratives, University Louis Pasteur, 67084 Strasbourg, France

Chromogranin A (CgA) has been proposed to play a major role in the formation of dense-core secretory granules (DCGs) in neuroendocrine cells. Here, we took advantage of unique features of the frog CgA (fCgA) to assess the role of this granin and its potential functional determinants in hormone sorting during DCG biogenesis. Expression of fCgA in the constitutively secreting COS-7 cells induced the formation of mobile vesicular structures, which contained cotransfected peptide hormones. The fCgA and the hormones coexpressed in the newly formed vesicles could be released in a regulated manner. The N- and C-terminal regions of fCgA, which exhibit remarkable sequence conservation with their mammalian counterparts were found to be essential for the formation of the mobile DCG-like structures in COS-7 cells. Expression of fCgA in the corticotrope AtT20 cells increased pro-opiomelanocortin levels in DCGs, whereas the expression of N- and C-terminal deletion mutants provoked retention of the hormone in the Golgi area. Furthermore, fCgA, but not its truncated forms, promoted pro-opiomelanocortin sorting to the regulated secretory pathway. These data demonstrate that CgA has the intrinsic capacity to induce the formation of mobile secretory granules and to promote the sorting and release of peptide hormones. The conserved terminal peptides are instrumental for these activities of CgA.

Eukaryotic cells share the capacity to rapidly secrete proteins through the constitutive secretory pathway. The fundamental feature of neuroendocrine and endocrine cells is the occurrence

of dense-core secretory granules (DCGs),<sup>3</sup> which are key cytoplasmic organelles responsible for secretion of hormones, neuropeptides, and neurotransmitters through the regulated secretory pathway (RSP). Storage at high concentrations of these secretory products is required for their finely tuned release in response to extracellular stimulation (1, 2). DCG biogenesis starts with the budding of immature secretory granules (ISGs) from the *trans*-Golgi network (TGN) through interactions between lipid rafts and protein components, in a similar manner to constitutive vesicle budding (2, 3). The ISG budding is followed by a multistep maturation process to form the mature secretory granules, including removal of the constitutive secretory proteins and lysosomal enzymes inadvertently packaged into ISGs (4).

Despite increasing knowledge of the various steps of DCG formation, the nature of the sorting signals for entry of proteins into the DCGs and the molecular machinery required to generate secretory granules are not fully elucidated (5, 6). Several recent studies highlighted the role of members of the granin family, which may represent the driving force for granulogenesis in the TGN (2), although this notion has been a matter of debate (7). Granins are soluble acidic proteins widely distributed in endocrine and neuroendocrine cells, which are characterized by the ability to aggregate at acidic pH and a high Ca<sup>2+</sup> environment (8, 9). These conditions are found in the lumen of the TGN allowing granins to aggregate in this compartment and to be segregated from constitutively secreted proteins (10, 11). The granin aggregates are believed to associate directly or indirectly with lipid rafts at the TGN to induce budding and formation of the ISGs. A prominent role of chromogranin A (CgA) in the regulation of DCG formation in endocrine and

\* This work was supported by INSERM, the Conseil Régional de Haute-Normandie, the COMETE-3 Network (Grant PHRC AOM-06179), the Ministère des Affaires Etrangères, and the Ministerio de Educacion y Ciencia (Grant HF2005-0053).

† The on-line version of this article (available at <http://www.jbc.org>) contains supplemental Videos S1–S8.

‡ Both authors contributed equally to this work.

¶ To whom correspondence should be addressed. Tel.: 33-235-14-66-61; Fax: 33-235-14-69-46; E-mail: [youssef.anouar@univ-rouen.fr](mailto:youssef.anouar@univ-rouen.fr).

<sup>3</sup> The abbreviations used are: DCG, dense-core secretory granule; RSP, regulated secretory pathway; ISG, immature secretory granule; TGN, *trans*-Golgi network; CgA, chromogranin A; fCgA, frog CgA; POMC, pro-opiomelanocortin; ACTH, adrenocorticotropin; GFP, green fluorescent protein; GH, growth hormone; VAMP2, vesicle-associated membrane protein-synaptobrevin; NPY, neuropeptide Y; MBP, maltose-binding protein; TBS, Tris-buffered saline; TBS-T, Tween 20 containing TBS; PBS, phosphate-buffered saline.

neuroendocrine cells has been proposed. Thus, depletion of CgA in PC12 cells led to a dramatic decrease in the number of DCGs (12), and exogenously expressed CgA in these depleted PC12 cells, as in DCG-deficient endocrine A35C and 6T3 cells, restored DCG biogenesis (12, 13). Besides, expression of granins in non-endocrine, constitutively secreting cells such as CV-1, NIH3T3, or COS-7 cells provoked the formation of DCG-like structures that release their content in response to  $\text{Ca}^{2+}$  influx (12, 14, 15). Further investigations performed in CgA null mice and transgenic mice expressing antisense RNA against CgA also revealed a reduction in the number of DCGs in chromaffin cells that was associated with an impairment of catecholamine storage, thus demonstrating the crucial role of CgA in normal DCG biogenesis (16, 17). In CgA knockout mice, the introduction of the gene expressing human CgA restored the regulated secretory phenotype (16). A different CgA null mice strain exhibited no discernable effect on DCG formation, but elevated catecholamine secretion (18), proving that CgA deficiency is associated with hormone storage impairment in neuroendocrine cells *in vivo*, a finding that was confirmed *in vitro* (19). The CgA<sup>-/-</sup> mice strain generated by Hendy *et al.* (18) exhibited a compensatory overexpression of other granins, pointing to a possible overlap in granin function in secretory granule biogenesis.

We reported previously that the frog CgA (fCgA) gene is coordinately regulated with the pro-opiomelanocortin (POMC) gene in the pituitary pars intermedia during the neuroendocrine reflex of skin color change, which allows amphibia to adapt to their environment through the release of POMC-derived melanotropic peptides (20, 21). Sequence comparison of fCgA with its mammalian orthologs revealed a high conservation of the N- and C-terminal domains, and far less conservation of the central part of the protein (Fig. 1A), suggesting that these domains may play a role in DCG formation and hormone release in various species (9, 20, 21). To assess the role of fCgA and its conserved N- and C-terminal regions in hormone sorting, storage, and secretion, we engineered different constructs that produce the native unmodified (no tag added) protein and truncated forms lacking the conserved N- and C-terminal domains, and we developed an antibody that specifically recognizes the central region of fCgA. Using the constitutively secreting COS-7 cells, which are devoid of DCGs, we could demonstrate for the first time that CgA is essential for targeting peptide hormones to newly formed mobile DCG-like structures. In the CgA-expressing AtT20 cells, which exhibit an only moderate capacity to sort secretory proteins to the regulated pathway (22), the granin plays a pivotal role in the sorting and release of POMC. The conserved terminal peptides of CgA are instrumental for these activities.

## EXPERIMENTAL PROCEDURES

**Antibodies and Reagents**—Primary antibodies used were: rabbit polyclonal anti-human WE14 at 1:1000 (23); sheep anti-human adrenocorticotropin (ACTH) (24) at 1:1000 for immunofluorescence and 1:500 for Western blot; goat anti-human pancreatic at 1:100 and goat anti-human lamp-1 at 1:100 (Santa Cruz Biotechnology, Santa Cruz, CA); mouse monoclonal anti-green fluorescent protein (GFP) at 1:250 (Roche

Diagnostics, Mannheim, Germany), mouse monoclonal GM130 antibodies at 1:1000 (BD Biosciences, Le Pont de Claix, France), and rabbit polyclonal anti-growth hormone (GH) at 1:200 (Dr. A. F. Parlow, National Hormone and Pituitary Program, NIDDK, Torrance, CA). For immunofluorescence, secondary antibodies were: Alexa 594-conjugated donkey anti-rabbit and Alexa 594-conjugated goat anti-mouse immunoglobulins (IgG), Alexa 488-conjugated donkey anti-goat IgG and Alexa 488-conjugated donkey anti-sheep IgG, at 1:300 (Invitrogen). For Western blot, anti-rabbit (Amersham Biosciences, Courtaboeuf, France) or anti-sheep (Jackson ImmunoResearch) horseradish peroxidase-conjugate secondary antibodies were used at 1:1000. For electron microscopy, rabbit secondary antibody conjugated to 10-nm gold particles (British Biocell, Tebu, France) was used at 1:20. GFP-tagged vesicle-associated membrane protein-synaptobrevin (VAMP2-GFP) and Venus-tagged neuropeptide Y (NPY-Venus) were gifts from R. W. Holz (University of Michigan, Ann Arbor) and D. Perrais (CNRS UMR 5091, Bordeaux, France), respectively.

**Production of Recombinant fCgA<sub>107–234</sub> and the Cognate Antibody**—A cDNA sequence encoding portion of the central region of fCgA was amplified by PCR from the fCgA cDNA (20) using 50 pmol of the sense primer 5'-ATGCGAATTCCGTCT-TCACAGTTAAATTC-3' and the antisense primer 5'-ATG-CAAGCTTAAATCCTCATCGAATTGTC-3'. An EcoRI restriction site necessary for subcloning was incorporated at the 5'-end of the sense primer. A stop codon and a HindIII restriction site necessary for the production of the protein and for subcloning, respectively, were introduced at the 5'-end of the antisense primer. The PCR product was digested with EcoRI and HindIII, and ligated to the expression plasmid pMAL-c2 (New England Biolabs, Beverly, MA) previously cut with EcoRI and HindIII. The construct was verified by DNA sequencing. This strategy allows for the subcloning of fCgA<sub>107–234</sub> cDNA in the sense orientation, in-frame with and downstream of the plasmid region encoding the bacterial maltose-binding protein (MBP). The MBP-fCgA<sub>107–234</sub> fusion protein was expressed in isopropyl 1-thio-β-D-galactopyranoside-induced *Escherichia coli* and affinity purified from bacterial soluble extracts applied to amylose resin essentially as described by the manufacturer of the Protein Fusion and Purification System (New England Biolabs). Antibodies (RV31.4) against the fusion protein were raised by injecting New Zealand rabbits. Sera from the immunized rabbits were used at 1:1000 for electron microscopy and at 1:500 for immunofluorescence and Western blot analysis to immunostain full-length and truncated forms of fCgA.

**Construction of Expression Vectors**—Full-length fCgA and the C-terminal deletion mutant fCgA<sub>1–336</sub> (named ΔCfCgA) were obtained by PCR cloning using the sense primer FCCA-1 (5'-TGCGATATCCAGCCAGCCGGATCC-3'), including an EcoRV restriction site (underlined bases), and the antisense primer FCCA-5 (5'-ATGCGCGGCCGCTCATCCCCTCCTCAA-3'), including a NotI restriction site. To produce the N-terminally deleted form of fCgA, *i.e.* fCgA<sub>76–378</sub> (named ΔNfCgA) and the N/C-terminally deleted fCgA, *i.e.* fCgA<sub>76–336</sub> (named ΔNCfCgA), the corresponding cDNAs were amplified by PCR using the sense primer FCCA-4 (5'-ATGCGAAT-TCAAGAAGAACTCGCGGC-3'), including EcoRI restriction

## Frog CgA Promotes Hormone Sorting

site, and the antisense primer FCCA-2 (5'-ATGCGCGGC-CGCTTATCTTCTGGCCTTTG-3') or FCCA-5, including the NotI restriction site. The amplified fragments were digested with the appropriate enzymes and subcloned into the eukaryotic expression vector pIREsneo2 plasmid (BD Clontech, Saint Germain-en-Laye, France). Because the N terminally deleted forms of fCgA would lack a signal peptide, we amplified this sequence from fCgA cDNA using the sense primer FCCA-1 and the antisense primer FCCA-3 (5'-ATGCGAATTCAG-GAAGGGACAAACTTGTGC-3'), including EcoRI restriction site, and inserted it upstream of the cDNAs encoding these proteins. PCR was performed in a GeneAmp PCR system 9700 (PerkinElmer Life Sciences). All the constructs were verified by restriction enzyme digestion and nucleotide sequence analysis using a Li-Cor 4200 DNA sequencer (Science Tec, Les Ulis, France).

**Cell Culture and Transfection**—African green monkey kidney fibroblast-derived COS-7 cells (ATCC, CRL 1651), and mouse corticotrope-derived AtT20/D16v-F2 cells (ATCC, CRL1795) were maintained in Dulbecco's modified Eagle's medium (Sigma-Aldrich) supplemented with 10% heat-inactivated fetal bovine serum (Sigma-Aldrich), 100 units ml<sup>-1</sup> penicillin, and 100 µg ml<sup>-1</sup> streptomycin (Invitrogen) at 37 °C in 5% CO<sub>2</sub>. Supercoiled plasmid DNA for transfection was purified on Qiagen columns. Cells were transfected with 0.8 µg (24-well plate) or 1.25 µg (12-well plate) of DNA constructs and 1–2 µl of Lipofectamine 2000 (Invitrogen) per well according to the manufacturer's protocol. Six hours after the beginning of transfection, the culture medium was replaced, and cells were further cultured for 48 h.

**Secretion Analysis**—Transiently transfected COS7 cells cultured in 24-well Costar plates were extensively washed with secretion medium (150 mM NaCl, 5 mM KCl, 2 mM CaCl<sub>2</sub>, 10 mM HEPES, pH 7.4) and subsequently incubated in this medium alone (constitutive release) or with the Ca<sup>2+</sup> ionophore A23187 (1 µM, Sigma, stimulated release of NPY) for 30 min or in barium secretion buffer (150 mM NaCl, 5 mM KCl, 2 mM BaCl<sub>2</sub>, 10 mM HEPES, pH 7.4) (stimulated release of GH) for 15 min, at 37 °C in 5% CO<sub>2</sub>. Transiently transfected AtT20 cells grown in 24-well Costar plates were extensively washed with secretion medium (150 mM NaCl, 5 mM KCl, 10 mM HEPES, pH 7.4), and subsequently incubated in secretion medium (constitutive release) or in potassium secretion medium (85 mM NaCl, 59 mM KCl, 2 mM CaCl<sub>2</sub>, 10 mM HEPES, pH 7.4) (stimulated release), for 1 h at 37 °C in 5% CO<sub>2</sub>. Secretion media were collected, cleared by centrifugation (5 min, 6,000 × g, 4 °C) and stored for further analysis. Cells were lysed in a buffer containing 50 mM Tris-HCl (pH 7.4), 10 mM NaCl, 5 mM EDTA, 1% Triton X-100, 1 mM dithiothreitol, and protease inhibitor mixture (Sigma), and centrifuged 20,000 × g for 15 min at 4 °C. Proteins in secretion media and cell homogenates were precipitated using 10% trichloroacetic acid and analyzed by Western blotting. For the GH release experiments, the cells were harvested by scraping in 10 mM PBS. The amounts of GH secreted into the medium and retained in the cells were measured using an enzyme-linked immunosorbent assay (Roche Applied Science). GH secretion is expressed as a percentage of total GH present in the cells before stimulation. For the ACTH

release experiments, the cells were harvested by scraping in 10 mM PBS. The amounts of ACTH secreted into the medium and retained in the cells were measured using an enzymatic immunoassay (Phoenix Pharmaceuticals, Burlingame, CA). ACTH secretion is expressed as a percentage of total ACTH present in the cells before stimulation.

**SDS-PAGE and Western Blot Analysis**—Proteins were separated by SDS-PAGE on 10% polyacrylamide gels in denaturing conditions and electroblotted onto nitrocellulose sheets (Amersham Biosciences). Membranes were incubated in a blocking buffer containing 5% non-fat dry milk in Tris-buffered saline (TBS) containing 0.05% Tween 20 (TBS-T) (Sigma) for 1 h at room temperature, incubated overnight with anti-fCgA, anti-WE14, anti-GFP, or anti-ACTH antibodies. Then, membranes were washed for 45 min with TBS-T. Blots were subsequently incubated for 1 h with appropriate secondary antibodies in blocking buffer. Immunoreactive proteins were detected by chemiluminescence (Amersham Biosciences). The radiographs were analyzed with a computer-assisted image analyzer (Biocom 2000, Les Ulis, France).

**Immunofluorescence Microscopy**—All procedures in this study conformed to the animal welfare guidelines of the European Community and were approved by the French Ministry of Agriculture (authorization no. 76.451). Frogs were anesthetized by immersion in a solution of 0.1% triaminobenzoic acid ethyl ester (Sigma-Aldrich) and perfused transcardially with 100 ml of PBS. The perfusion was continued with 100 ml of Stefanini's fixative (4% paraformaldehyde, 0.2% picric acid). Rats were anesthetized with an intraperitoneal injection of sodium pentobarbital (35 mg/kg) and perfused through the aorta with 50 ml of PBS followed by 300 ml of Stefanini's fixative. The adrenal glands and pituitaries were quickly dissected and post-fixed overnight at 4 °C with the same fixative solution. The glands were stored in 15% sucrose in PBS for 12 h and transferred into PBS containing 30% sucrose. Then, they were placed in an embedding medium (OCT Tissue Teck, Nussloch, Germany) and immediately frozen. The tissues were cut in 10-µm sections using a cryomicrotome (Frigocut 2800 E, Reichert Jung, Nussloch, Germany). Cells cultured onto poly-L-lysine (Sigma-Aldrich)-coated glass coverslips were transfected as described above and fixed with 4% paraformaldehyde in PBS at room temperature for 10 min. Tissue slices and cells were permeabilized for 20 min with 0.3% Triton X-100 in PBS and treated with normal donkey serum at 1:100 dilution to reduce nonspecific antibody labeling. Biological samples were then incubated for 2 h at room temperature with one or two unlabeled primary antibodies, and for 1 h with one or two secondary antibodies. Tissue slices and cells were observed on a Leica SP2 upright confocal laser scanning microscope (DMRAX-UV) equipped with the Acousto-Optical Beam Splitter system and with 25×, 40×, and 63× oil immersion objectives (Leica, Microsystems, Reuil-Malmaison, France). For confocal images, Alexa 488 was excited at 488 nm and observed in a 505–540 nm window. Alexa 594 was excited at 594 nm and observed in a 600–630 nm window. Overlay and maximum projection of the z-stacks files have been performed with post acquisition Leica confocal software functions to obtain the presented snapshots. To verify the

specificity of the immunoreaction, the primary or secondary antibodies were substituted with PBS.

**Immunoelectron Microscopy and Morphometry**—COS-7 cells were cryofixed using an EM-PACT I High Pressure Freezing apparatus (Leica) without any precooling treatment and freeze-substituted using the freeze-substitution apparatus (AFS, Leica) in anhydrous acetone containing 0.5% uranyl acetate. The substitution procedure was as follows: −90 °C for 72 h, −60 °C for 12 h, −30 °C for 12 h, and finally −15 °C with increasing temperature steps of 2 °C/h. Samples were washed twice in anhydrous ethanol to remove acetone and embedded at −15 °C in a solution containing ethanol/London Resin White (ratios of 2:1, 1:1, and then 1:2 for 8 h for each step) and in pure resin for 24 h twice. Polymerization was carried out at −15 °C under UV light for 48 h, within the AFS apparatus. All incubations were carried out at room temperature. Ultrathin sections (50–70 nm) mounted on carbon-Formvar-coated nickel grids were incubated in the blocking solution containing TBS supplemented with 0.2% acetylated bovine serum albumin and 0.05% Tween 20 for 15 min. The grids were then incubated with the primary fCgA antibody diluted 1:1000 in TBS containing 0.2% acetylated bovine serum albumin and 3% normal goat serum for 2 h. After washing in TBS with 0.2% acetylated bovine serum albumin, grids were incubated for 90 min with an anti-rabbit secondary antibody conjugated to 10 nm colloidal gold particles diluted 1:20 in the same buffer as the primary antibody. After washing, grids were transferred to a droplet of TBS containing 2% glutaraldehyde for 10 min and rinsed in TBS followed by deionized water. Sections were stained with uranyl acetate (0.5% in methanol) and lead citrate for 10 min. Observations were made at 80 Kv in a Tecnai 12 Biotwin electron microscope (FEI Co., Eindhoven, Netherlands). Image acquisitions were performed with a charge-coupled device Megaview II camera controlled by AnalySis software (Eloise, Paris, France). Control for the specificity of CgA immunogold labeling included omitting primary antibody and using non-transfected COS-7 cells or cells transfected by the empty vector (pIRES). Measurements of the diameter of newly formed DCG-like structures in cells transfected with fCgA were performed only on vesicles exhibiting labeling with fCgA antibody using AnalySis software. Mean size was determined from 98 values.

**Real-time Video Microscopy**—For imaging of living COS-7 cells, transfected cells were cultured in Labtec (Invitrogen) during 48 h at 37 °C in a controlled atmosphere (5% CO<sub>2</sub>) and examined under an inverted microscope (Leica) equipped with an incubation chamber (Solent Scientific Ltd., Segensworth, UK) and computer-controlled motorized stage and illumination shutters. Images were acquired with a 63× oil immersion objective and a CoolSnapfx camera (Princeton Instrument, Trenton, NJ) with a pixel size of 6.7 μm × 6.7 μm. The speed of image acquisition was three frames/s (2 × 2 binning). Images containing a region of interest within the cell were streamed to memory on a computer during acquisition and saved to a disk. Distance covered by each vesicle from its origin was analyzed by using Metamorph software (Molecular Devices, Saint-Greゴire, France). For analysis of single events, each acquired sequence (91 frames) was reviewed multiple times on screen at various settings of intensity to pick out all visible events. Meas-

urements were performed on entire cells, and only a small region of interest was used to illustrate vesicle trajectory.

**Quantification of Fluorescence Distribution**—Three-dimensional blind deconvolution of confocal images was performed using two iterations operated by Autoquant X software (Media-Cybernetics, Bethesda, MD). Deconvolved confocal images were analyzed and three-dimensional rendered by using Imaris software (Bitplane, Zurich, Switzerland). Fluorescent particles with a diameter > 200 nm were outlined and counted automatically. All three-dimensional reconstructions were done with the same threshold settings. For each three-dimensional image, 0.304-μm step z-stacks (512 × 512 focal planes) were acquired by using a 63× objective.

**Data Analysis**—Data are reported as mean values ± S.E. The non-parametric Mann-Whitney *U* test was used. Probability values less than 0.05 were considered significant. Data were analyzed with the Prism program (GraphPad Software, San Diego, CA).

## RESULTS

**Expression of fCgA Induces the Biogenesis of Dense-core Vesicles in Non-endocrine Cells**—To study native unmodified fCgA in endocrine and non-endocrine cells, we first developed an antibody that recognizes fCgA but not the mammalian CgA. Because the central region of fCgA exhibited very weak sequence similarity with its mammalian counterparts, we took advantage of this property to develop a specific antibody against the frog protein, using the recombinant polypeptide fCgA<sub>107–234</sub> (Fig. 1A). As shown in Fig. 1B, this antibody recognized CgA and its processing intermediates in frog pituitary extracts, but not in rat pituitary extracts. By contrast, an antibody directed against the conserved CgA-derived peptide WE14 detected CgA and its processing products in both rat and frog pituitary extracts (Fig. 1B). Using confocal microscopy, the antibody against fCgA revealed immunoreactive cells in frog pituitary and adrenal glands (Fig. 1C). In contrast, this antibody failed to label chromaffin cells in rat adrenal gland, which could be labeled only with the WE14 antibody (Fig. 1C). Thus, the antibody developed against fCgA provides a means to track specifically the frog CgA protein.

Previous studies have shown that expression of granins is sufficient to induce the appearance of secretory granule-like vesicles in non-endocrine cells (12, 14, 15). To assess the granulogenic activity of fCgA, we transfected COS-7 cells, which are devoid of a RSP, with fCgA cDNA or the empty vector, and analyzed the ultrastructure of these cells. Electron microscopy examination revealed that fCgA expression induces the formation of dense-core granular structures with a mean diameter of 330 ± 96 nm (*n* = 98) (Fig. 2A). These vesicles were immunolabeled with the anti-fCgA, indicating that fCgA is stored into the secretory granule-like organelles (Fig. 2A). In contrast, COS-7 cells transfected with the empty vector were devoid of such vesicular structures and did not show any CgA immunolabeling, adding another level of confidence to the specificity of the antibody used (Fig. 2B). To further characterize the fCgA-induced structures, we assessed in COS-7 cells the colocalization of fCgA with different vesicular markers, using specific antibodies directed against the lysosomal and late endosomal

## Frog CgA Promotes Hormone Sorting

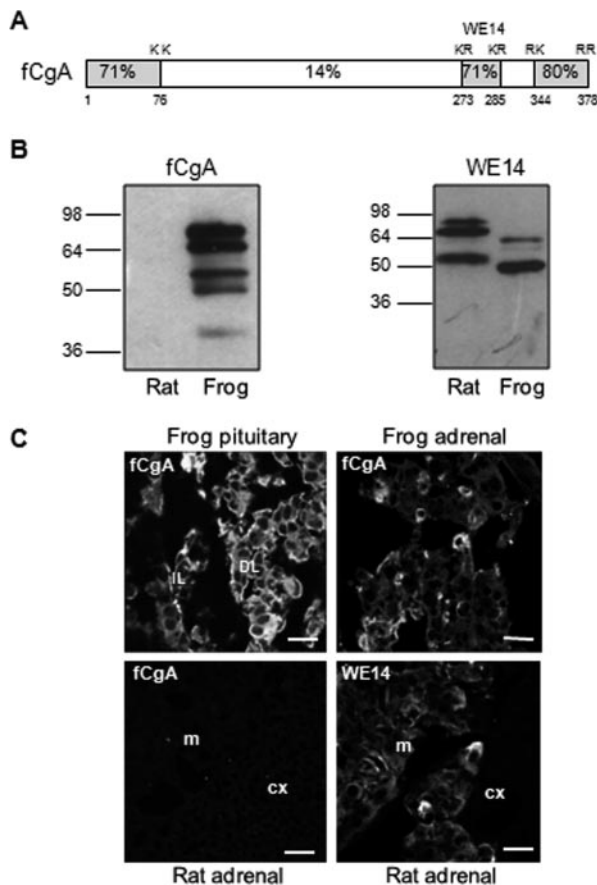


**FIGURE 1.** Specificity of the antibody directed against frog CgA. *A*, scheme depicting the structure of fCgA and showing the high conservation of the terminal regions and the percentages of amino acid identity between frog and human CgA sequences. The highly conserved peptide WE14 and dibasic cleavage sites are also indicated. *B*, Western blot showing that the antibody developed against fCgA recognized the protein and several processing intermediates in frog but not rat pituitary extracts, whereas an antibody, directed against the WE14 conserved peptide, detected CgA and its processing products in both rat and frog pituitary extracts. *C*, immunofluorescence analysis of frog pituitary and adrenal glands, and rat adrenal gland using the antibodies against fCgA and WE14. cx, cortex; DL, distal lobe; IL, intermediate lobe; and m, medulla. Scale bars equal 10  $\mu$ m.

protein lamp-1 or GH, and the fluorescently tagged fusion protein NPY-Venus. The antibody against lamp-1 stained numerous vesicular structures throughout the cytoplasm (Fig. 3*A*). Lamp-1-labeled vesicles did not show any fCgA immunoreactivity and vice versa (Fig. 3*A*), indicating that the fCgA-containing vesicles are not lysosomes/endosomes. By contrast, transfected NPY-Venus and GH colocalized with fCgA in most vesicular structures (Fig. 3, *B* and *C*). These data demonstrate that fCgA induces the biogenesis of granules with core-density and appropriate size and containing RSP proteins but not a lysosomal/endosomal protein.

**Frog CgA Is Required for the Targeting of RSP Proteins to Mobile Secretory Granule-like Structures**—Motion is an important property of secretory granules, which allows them to reach the plasma membrane to undergo exocytosis after a  $\text{Ca}^{2+}$  stimulus (25). To address the dynamics of the vesicular structures generated in COS-7 cells, fluorescence videomicroscopy of living cells was carried out after transfection of fluorescent RSP components in the absence or presence of fCgA. Expression of NPY or VAMP2/synaptobrevin fluorescent proteins in COS-7

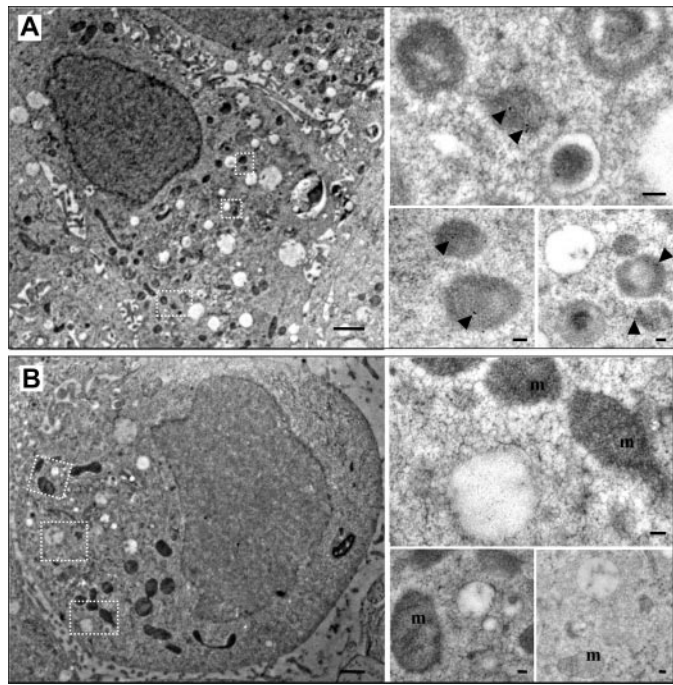


**FIGURE 2.** Frog CgA expression induces the biogenesis of secretory granule-like structures in COS-7 cells. Immunogold electron microscopy of COS-7 cells transfected with pIRES-fCgA (*A*) or with the empty vector (*B*). Scale bars equal 1  $\mu$ m. Insets show dense-core vesicles containing the protein (arrowheads) in fCgA-expressing cells and unlabeled organelles such as mitochondria in empty vector-transfected cells. Scale bars equal 100 nm. m, mitochondria; N, nucleus.

cells induced the appearance of protein accumulations throughout the cytoplasm (Fig. 4*A*), in agreement with the data reported by Beuret *et al.* (15) showing that various RSP proteins accumulate in granular structures in transfected COS-1 fibroblast cells. Automatic computer tracking showed that the formed aggregates were immobile (Fig. 4, *A* and *C*; *videos 1* and *2* in supplemental data), and that treatment with the  $\text{Ca}^{2+}$  ionophore A23187 (1  $\mu$ M, 10 min) did not virtually alter the behavior of these accumulations (Fig. 4, *B* and *C*; *videos 3* and *4* in supplemental data). In contrast, coexpression of these proteins with fCgA in COS-7 cells resulted in the biogenesis of vesicles that exhibited rapid movements, along with others that were immobile (Fig. 5, *A* and *C*; *videos 5* and *6* in supplemental data). Upon exposure to the ionophore A23187, no more mobile structures were observed and some stationary vesicles disappeared (Fig. 5, *B* and *C*, *videos 7* and *8* in supplemental data). Thus, although several proteins of the RSP trigger the formation of vesicular structures in non-endocrine cells, CgA expression is necessary for the biogenesis of secretory granule-like vesicles endowed with mobility and apparent exocytic ability in response to  $\text{Ca}^{2+}$  stimulation.

**Frog CgA Facilitates the Regulated Secretion of Co-stored Hormones**—Because the vesicles triggered by fCgA expression exhibited several similarities with *bona fide* secretory granules, we first quantified the secretion of fCgA from transfected COS-7 cells treated or not with the  $\text{Ca}^{2+}$  ionophore A23187. Normalized fCgA release in the medium relative to total CgA (medium plus cell content) was determined. Incubation of transfected cells with the ionophore (1  $\mu$ M) for 15–30 min

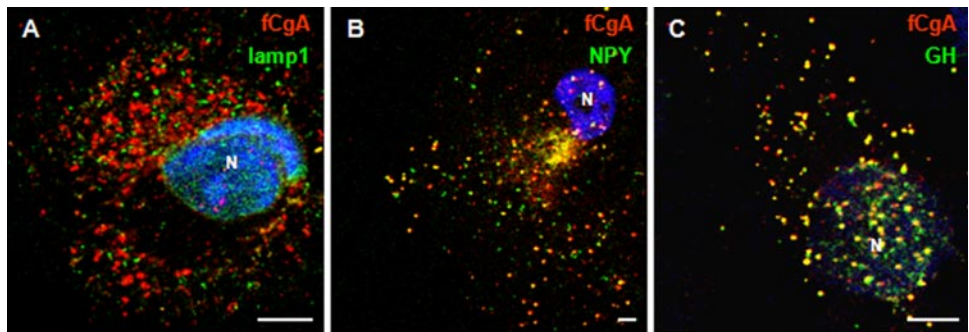


**FIGURE 3.** Double-fluorescence detection of fCgA and lamp-1 (A), NPY-Venus (B), or GH (C) in cytoplasmic vesicles. *N*, nucleus. Scale bars equal 5  $\mu$ m.

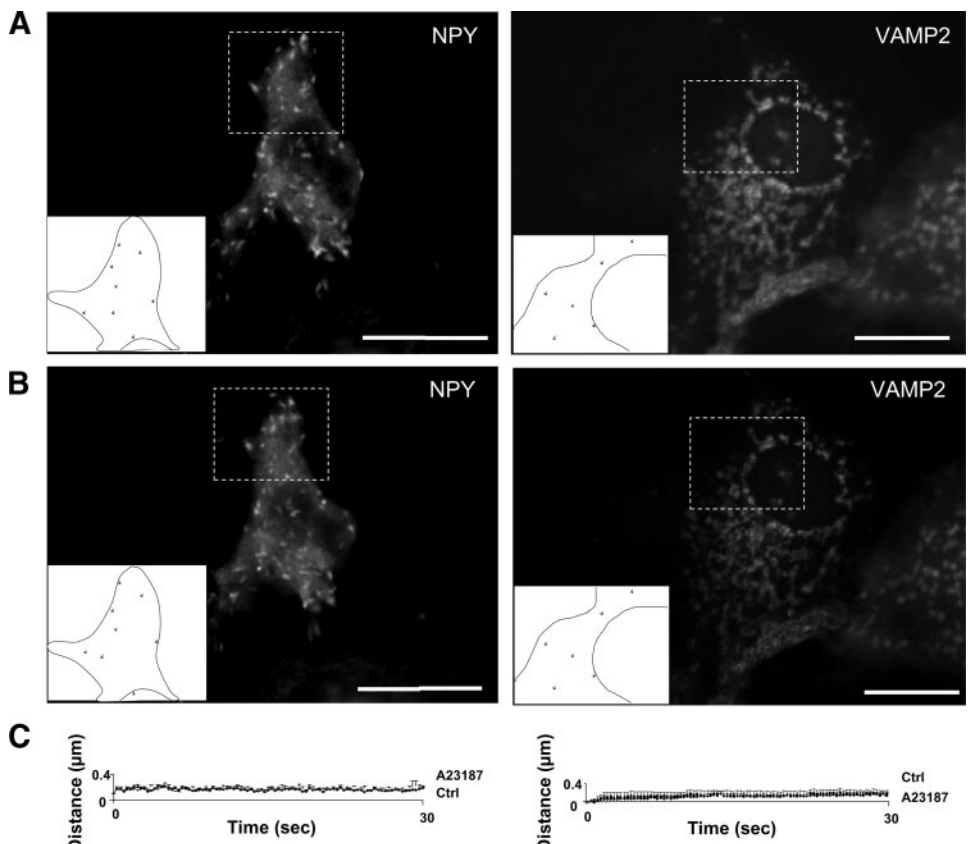


**FIGURE 4.** Tracking of NPY- and VAMP2-containing structures in transfected COS7 cells. *A* and *B*, COS-7 cells were transfected with NPY-Venus or VAMP2-GFP and imaged via live epifluorescence microscopy before (*A*) and after (*B*) treatment with the  $\text{Ca}^{2+}$  ionophore A23187 (1  $\mu$ m) for 10 min. Large tubular structures were observed in the cytosol and were tracked during 30 s (supplemental videos S1–S4). Composite images (boxes and insets) containing the tracked structures in portions of transfected cells are shown. *C*, plots of the distance covered from origin against time showing that the structures were immobile in control and stimulated conditions.

caused a significant increase in the amount of fCgA present in the culture medium (Fig. 6*A*), indicating that the protein stored could be released upon stimulation and that the structures formed are functional secretory vesicles. As fCgA oriented coexpressed NPY-Venus into mobile vesicular structures (see above), we next examined the relative release of NPY-Venus and GH when expressed in the absence or presence of fCgA in COS-7 cells. In the absence of fCgA, the immunoreactive proteins could be detected in the culture medium of COS-7 cells in basal as well as stimulated conditions with no discernable difference in concentration (Fig. 6, *B* and *C*). Coexpression of

NPY-Venus or GH with fCgA led to a sharp increase in the release of the peptides into the medium upon stimulation with A23187 or barium, respectively (Fig. 6, *B* and *C*), showing that fCgA is sufficient and necessary for the sorting and regulated secretion of a coexpressed hormone. Additionally, fCgA was more efficient in the sorting of NPY-Venus than GH to the RSP (Fig. 6, *B* and *C*).

*Deletion of the N- and C-terminal Peptides of fCgA Markedly Reduces Its Granulogenic Activity*—The frog and mammalian CgA exhibit remarkable sequence conservation at their N- and C-terminal regions (9, 20). We hypothesized that these discrete domains may represent important and ubiquitous determinants for the activity of CgA in granulogenesis in various species. To test this hypothesis, we used the fCgA cDNA to engineer different constructs that produce N-, C-, or N- and C-terminally truncated forms of the native protein (Fig. 7*A*) to determine the contribution of these conserved peptides to the granulogenic function of CgA. In COS-7 cells transfected with full-length fCgA, vesicular structures were formed throughout the cytoplasm, as revealed by confocal microscopy (Fig. 7*B*). Truncation of the conserved N- and/or C-terminal domains led to a drop in the number of granules formed, which was more pronounced when both peptides were deleted (Fig. 7*B*). In the latter case, CgA immunoreactivity was localized mostly in a perinuclear area, which coincided with GM130 Golgi marker labeling (Fig. 7*C*). These data indicate that the two terminal motifs are instrumental for

the role of CgA in triggering the biogenesis of secretory granule-like vesicles. To substantiate this notion, we analyzed the secretory properties of the cells transfected with the different fCgA constructs using Western blotting. These experiments revealed a notable increase in the relative concentration of full-length fCgA in the secretion medium after stimulation of COS-7 cells with the  $\text{Ca}^{2+}$  ionophore A23187 (1  $\mu$ m), whereas no apparent variation was observed in the release of the truncated forms of fCgA (Fig. 8*A*). These results demonstrate that both the N- and C-terminal conserved domains are important for the regulated secretion of CgA. To determine the influence

## Frog CgA Promotes Hormone Sorting

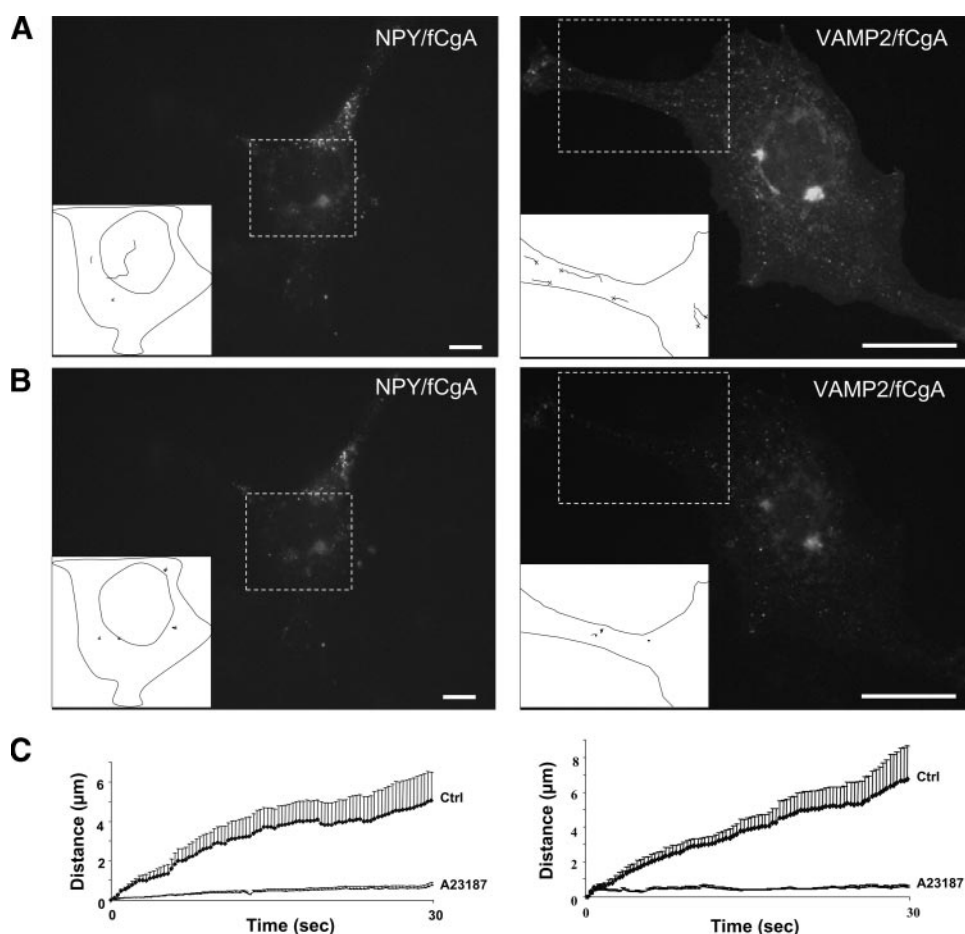


**FIGURE 5.** Frog CgA induces the biogenesis of mobile DCG-like structures. *A* and *B*, COS-7 cells were cotransfected with full-length fCgA and NPY-Venus or VAMP2-GFP, and imaged via live epifluorescence microscopy before (*A*) and after (*B*) treatment with A23187 (1 μM) for 10 min. Small vesicular structures were observed in the cytosol and were tracked during 30 s (supplemental videos S5–S8). Composite images (boxes and insets) containing the tracked vesicles in portions of transfected cells are shown. Few tracked vesicles moved rapidly before A23187 treatment but were essentially immobile after treatment (supplemental videos S5–S8). *C*, plots of the distance covered from origin against time for the vesicles tracked in control and stimulated conditions.

of these regions on the regulated secretion of NPY-Venus, we measured the release of this protein in the presence of fCgA or the various deletion mutants (Fig. 8*B*). In contrast to fCgA, the mutants were unable to regulate either the basal or the  $\text{Ca}^{2+}$  ionophore-stimulated secretion of NPY-Venus (Fig. 8*B*), indicating that the terminal peptides are also important for the regulated secretion of coexpressed hormones.

**Deletion of the Conserved Domains of fCgA Impairs Its Sorting to Secretory Granules in Endocrine Cells**—To examine the fate of fCgA and its mutant forms in the CgA-expressing AtT20 cells, we used the specific antibody generated against the frog protein. Confocal microscopy analysis of cells transfected with fCgA revealed a characteristic punctate labeling of secretory granules throughout the cytoplasm (Fig. 9*A*; see also Fig. 10*B*), indicating that the intact fCgA is correctly addressed in AtT20 cells. However, cells transfected with the N- and/or C-terminally deleted forms exhibited a marked decrease in the number of fCgA-positive granular structures (Fig. 9*A*), suggesting that the conserved domains of CgA are essential for targeting this protein to secretory granules in endocrine cells. Western blot analysis showed that fCgA and its truncated forms are pro-

duced in AtT20 cells, and that secretion of the mutant proteins is not significantly modified by 59 mM KCl stimulation (Fig. 9*B*). Finally, deletion of both the N- and C-terminal peptides provoked a significant decrease in the release of fCgA in basal condition (Fig. 9*B*). These findings highlight the importance of the conserved peptides for the sorting and secretion of CgA in endocrine cells.

**Deletion of the Conserved Peptides of fCgA Obliterates the Sorting of POMC to Secretory Granules**—To determine the importance of CgA conserved peptides in secretory cells, we examined POMC storage and release in the presence and absence of fCgA or derived truncated forms in AtT20 cells. Cell stimulation did not elicit the release of detectable amounts of POMC in non-transfected AtT20 cells (Fig. 10*A*). However, AtT20 cells transfected with fCgA released an appreciable amount of POMC after stimulation with 59 mM KCl (Fig. 10*A*), suggesting that overexpression of CgA enhances the pool of releasable POMC via the regulated pathway of secretion. This effect of CgA is abolished when its conserved N- and/or C-terminal peptides were removed (Fig. 10*A*). When cell contents were analyzed using Western blotting, no POMC immunoreactivity could be

detected in AtT20 cells in these conditions; however, when fCgA or its deletion mutants were expressed, POMC immunoreactivity could be seen in all conditions (Fig. 10*A*). This suggests that the POMC levels were increased in AtT20 cells upon expression of fCgA. The fact that POMC could also be detected in cells transfected with the truncated forms of fCgA indicates that the central highly acidic region of CgA is probably sufficient to increase intracellular POMC in AtT20 cells (Fig. 10*A*). In contrast to POMC, expression of fCgA or its molecular variants did not modify ACTH relative secretion in basal or stimulated condition (Fig. 10*B*).

To examine the effects of fCgA at the cellular level, we analyzed the distribution of this protein and its deleted forms in comparison to that of POMC in AtT20 cells. We first showed that fCgA colocalized with pancreastatin, a mammalian CgA-derived peptide that is absent in frog CgA sequence (20), indicating that fCgA and the endogenous CgA are sorted to the same secretory granules (Fig. 10*C*). Frog CgA and POMC immunoreactivities also coincided in the same granules (Fig. 10*C*). Interestingly, overexpression of CgA enhanced POMC immunoreactivity in the secretory granules (compare fCgA-

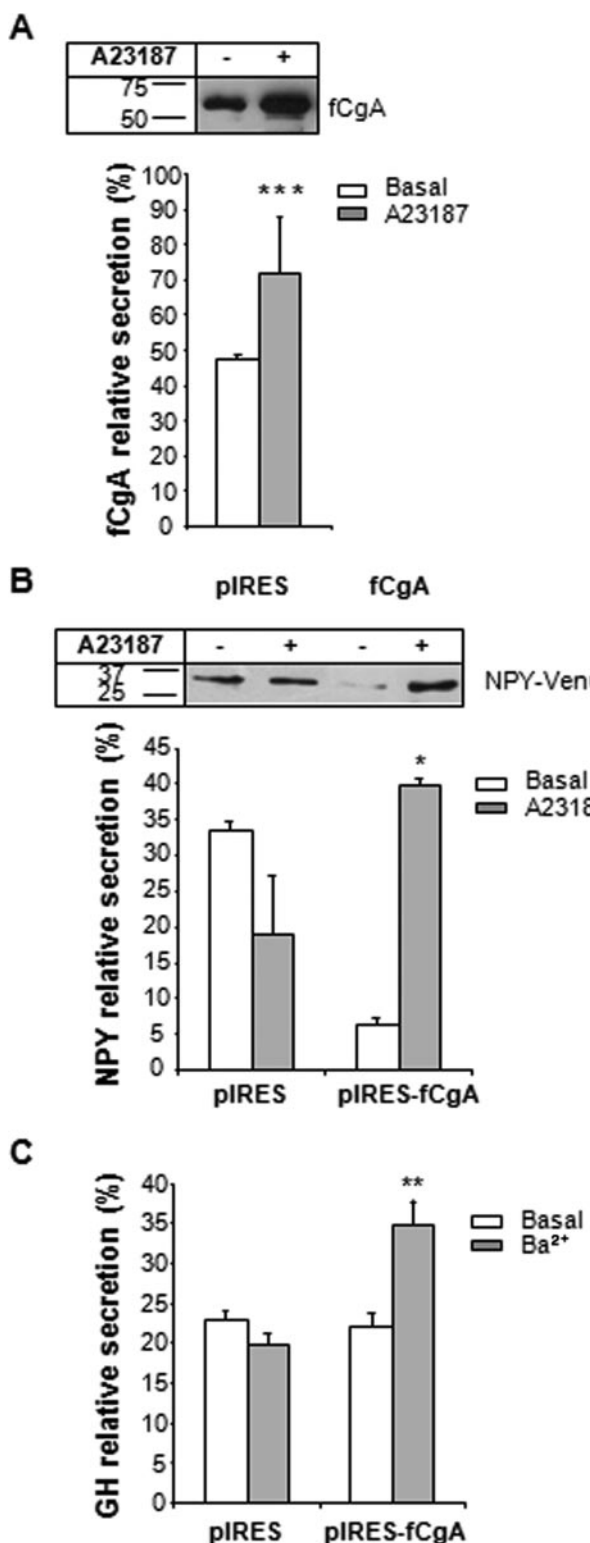


**FIGURE 6.** Regulated secretion in CgA-expressing COS-7 cells. *A*, Western blot analysis of COS-7 cells expressing fCgA treated or not with 1  $\mu$ M A23187 for 30 min. Approximately 50% of the release medium and 50% of the cell content were used for this analysis. The graph represents the mean values  $\pm$  S.E. of normalized fCgA release in the medium relative to total CgA (medium plus cell content) ( $n = 3$ ; \*\*\* $p < 0.001$ ). *B*, Western blot analysis of COS-7 cells expressing NPY-Venus in the absence or presence of fCgA and treated or not with 1  $\mu$ M A23187 during 30 min. The graph represents the mean values  $\pm$  S.E. of normalized NPY-Venus release in the medium relative to total NPY-Venus (medium plus cell content) ( $n = 3$ ; \* $p < 0.05$ ). Similar results were obtained after 15 min of stimulation with the  $\text{Ca}^{2+}$  ionophore. *C*, enzyme-linked

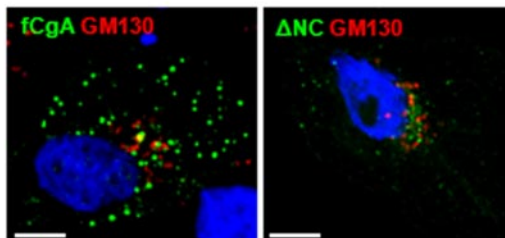
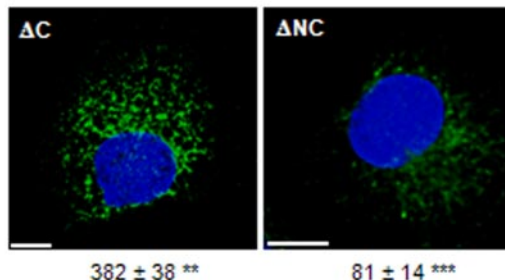
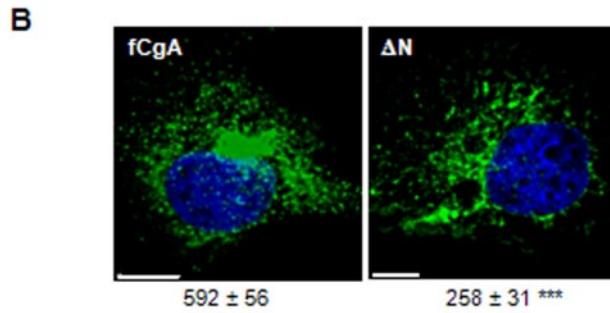
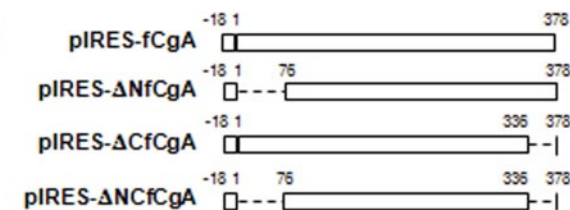


**FIGURE 7.** Deletion of the N- and/or C-terminal regions of fCgA markedly reduces its granulogenic activity in COS-7 cells. *A*, schemes depicting the different fCgA constructs used. *B*, COS-7 cells transfected with plasmids encoding full-length fCgA or fCgA-truncated forms were examined for fCgA immunoreactivity using confocal microscopy. Three-dimensional reconstructions of confocal stacks were used to quantify automatically the granules with a diameter  $> 200$  nm. Values for the number of granules/cell, indicated under each representative image, are given as the means  $\pm$  S.E. ( $n = 10$ ; \*\* $p < 0.01$ ; \*\*\* $p < 0.001$ ). Scale bars, 10  $\mu$ m. *C*, COS-7 cells were transfected with plasmids encoding full-length fCgA or N- and C-terminally deleted protein, and examined for fCgA and GM130 immunoreactivities using confocal microscopy. Scale bars, 10  $\mu$ m.

positive and -negative cells in Fig. 10C), in agreement with the Western blot data described above. Deletion of the N- and/or C-terminals of CgA resulted in the loss of secretory granule labeling not only with the antibodies directed against fCgA but also with those directed against POMC (Fig. 10C), with most of the immunoreactivity accumulating in the perinuclear area. These findings indicate that truncation of CgA terminal peptides impaired the sorting of the granin, but also that of POMC,

immunosorbent assay analysis of COS-7 cells expressing GH in the absence or presence of fCgA, and treated or not with 2 mM  $\text{BaCl}_2$  during 15 min. The graph represents the mean values  $\pm$  S.E. of normalized GH release in the medium relative to total GH (medium plus cell content) ( $n = 4$ ; \*\* $p < 0.01$ ).

## Frog CgA Promotes Hormone Sorting

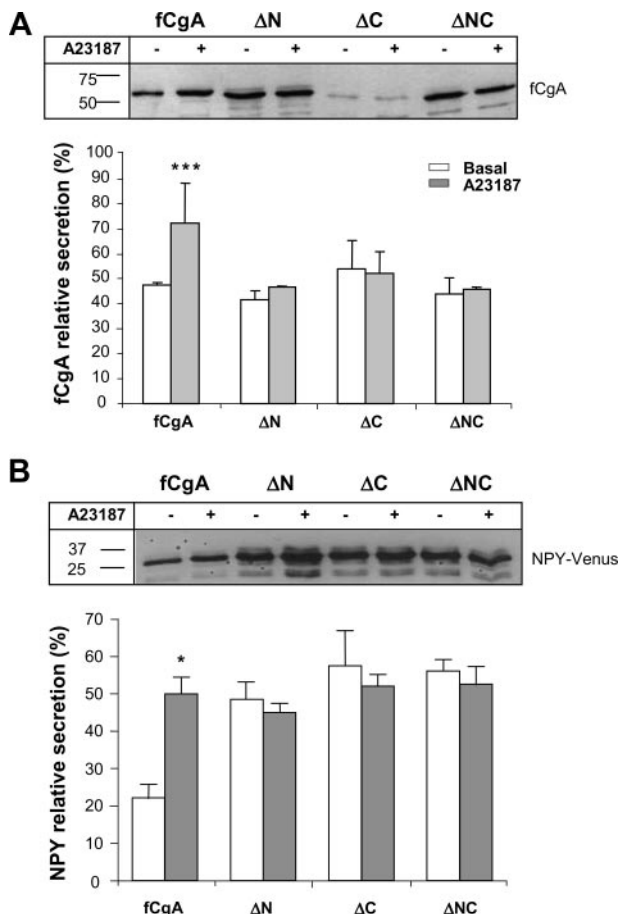


**FIGURE 8.** Deletion of the N- and/or C-terminal regions of fCgA abolishes the regulated secretion of cargo proteins in COS-7 cells. *A*, Western blot analysis of fCgA secretion in COS-7 cells treated or not with 1  $\mu$ M A23187 during 30 min. The graph represents the mean values  $\pm$  S.E. of normalized fCgA or deletion mutants release in the medium relative to total CgA (medium plus cell content) ( $n = 3$ ; \*\*\*,  $p < 0.001$ ). *B*, Western blot analysis of NPY-Venus secretion in COS-7 cells transfected with plasmids encoding full-length fCgA or fCgA-truncated forms, and treated or not with 1  $\mu$ M A23187 during 30 min. The graph represents the mean values  $\pm$  S.E. of normalized NPY-Venus release in the medium relative to total NPY-Venus (medium plus cell content) ( $n = 3$ ; \*,  $p < 0.05$ ).

leading to retention of these products in the Golgi area where the immunoreactivity of the two proteins was confined.

## DISCUSSION

Because CgA has been identified in DCGs of neuroendocrine and endocrine cells from phylogenetically distant species (9), this protein could represent a key regulator of hormone secretion and secretory granule biogenesis. Characterization of frog CgA and the observation that only the sequence of the N- and C-terminal regions of the protein has been conserved between frog and mammals (20), offered the unique opportunity to determine: (i) whether a CgA protein expressed in a phylogenetically distant species would also sustain a granulogenic activity, (ii) whether this activity would be harbored by specific functional determinants that would have been preserved through evolution, and (iii) whether this granulogenic activity would impinge on hormone sorting and secretion in constitutively and regulated secreting cell models. We demonstrated here that fCgA and its conserved N- and C-terminal peptides

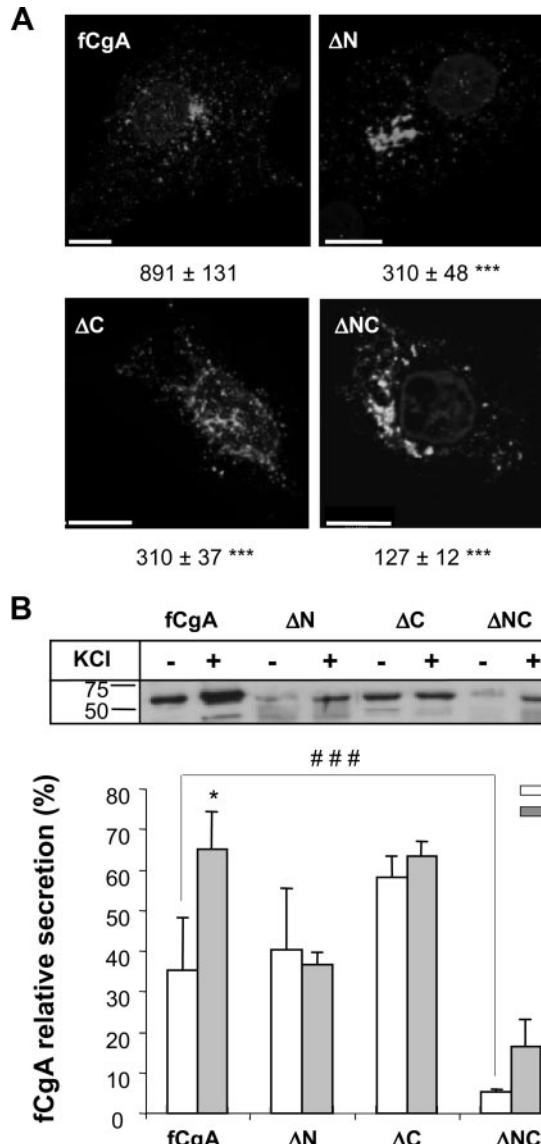


**FIGURE 9.** Terminal regions of fCgA are essential for its sorting to the regulated secretory pathway in AtT20 cells. AtT20 cells were transfected with full-length fCgA or fCgA-truncated forms and examined for fCgA immunoreactivity using confocal microscopy. Three-dimensional reconstructions of confocal stacks were used to quantify automatically the granules with a diameter  $> 200$  nm. Values for the number of granules/cell, indicated under each representative image, are given as the means  $\pm$  S.E. ( $n = 10$ ; \*\*\*,  $p < 0.001$ ). Scale bars, 10  $\mu$ m. *B*, Western blot analysis of fCgA secretion in AtT20 cells treated or not with 59 mM KCl during 1 h. The graph represents the mean values  $\pm$  S.E. of normalized fCgA or deletion mutants release in the medium relative to total CgA (medium plus cell content) ( $n = 3$ ; \*,  $p < 0.05$ ; # # #,  $p < 0.001$ ).

are not only important for promoting the biogenesis of *bona fide* mobile secretory granules, but also for the targeting and release of hormones through the RSP.

**Frog CgA Is Able to Generate Mobile Secretory Granule-like Structures Containing Peptide Hormones**—Different studies have demonstrated the ability of mammalian CgA to induce the formation of secretory granule-like structures in non-endocrine cells such as CV-1 (12), NIH3T3, and COS-7 (14) cells, which normally do not contain any secretory granules. Although frog CgA exhibits limited overall sequence identity with its mammalian orthologs, immunoelectron microscopy

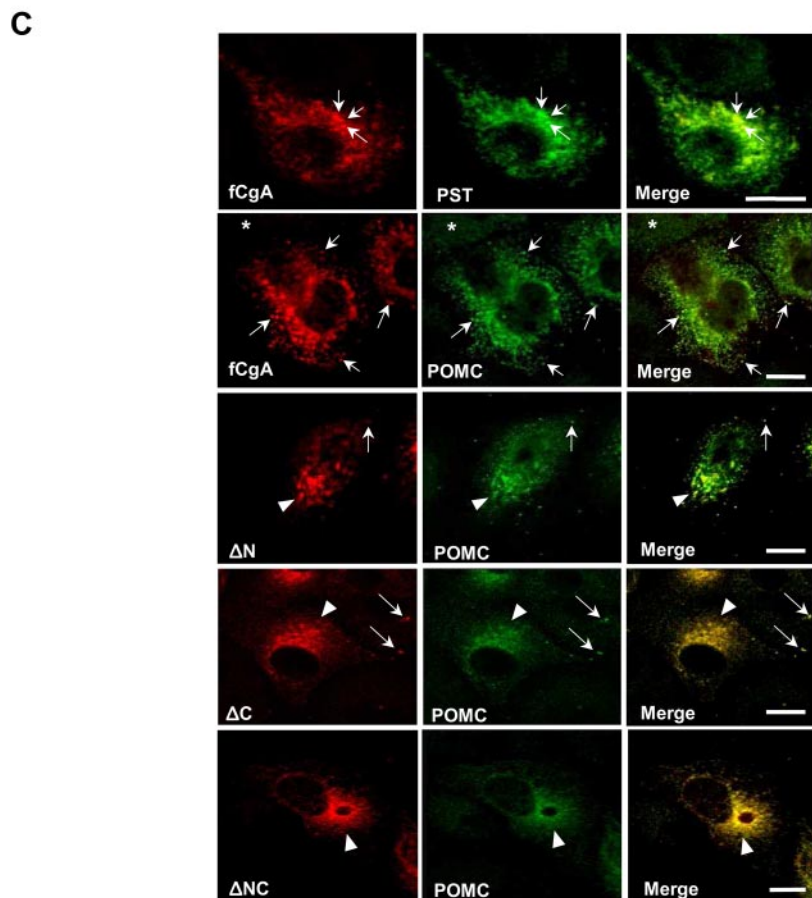
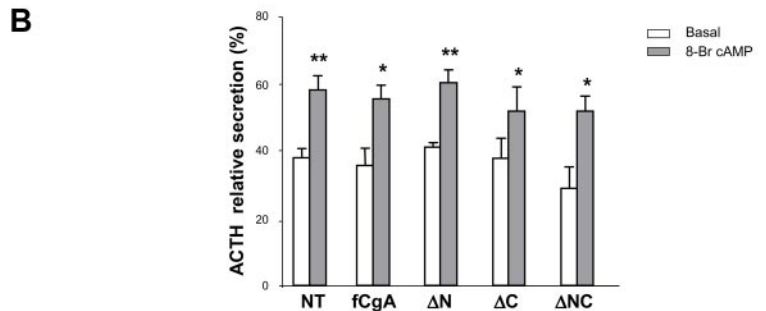
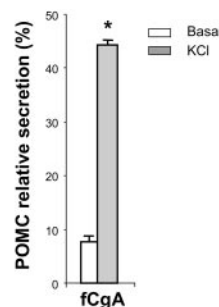
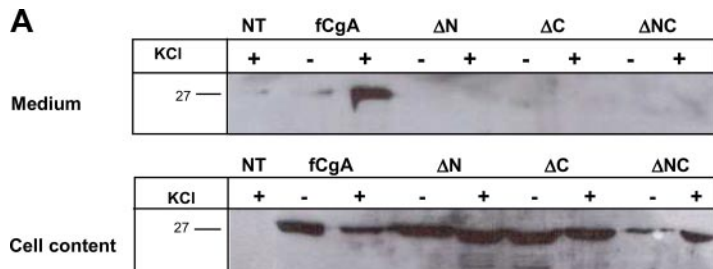


**FIGURE 10. Frog CgA directs POMC sorting, storage, and release through its conserved regions.** *A*, Western blot analysis of POMC secretion in AtT20 cells expressing fCgA or its truncated forms, and treated or not with 59 mM KCl during 1 h. The graph represents the mean values  $\pm$  S.E. of normalized POMC release in the medium relative to total CgA (medium plus cell content) ( $n = 3$ ; \* $p < 0.05$ ). NT, not transfected. *B*, enzyme immunoassay analysis of AtT20 cells expressing ACTH in the absence or presence of fCgA and its derived forms, and treated or not with 5 mM 8-Br-cAMP during 90 min. The graph represents the mean values  $\pm$  S.E. of normalized ACTH release in the medium relative to total ACTH (medium plus cell content) ( $n = 8$ ; \* $p < 0.05$ ; \*\* $p < 0.01$ ). *C*, AtT20 cells were transfected with full-length fCgA or fCgA-truncated forms and examined for pancreatic or POMC immunoreactivities using confocal microscopy. Arrows mark fCgA-positive vesicles. Arrowheads indicate the polarized staining in the perinuclear area. Asterisks show fCgA-negative (non-transfected), POMC-positive cells. Scale bars equal 20  $\mu$ m.

analysis showed that its expression in COS-7 cells induces the appearance of vesicles containing the protein, which display the characteristics of authentic DCGs proposed by Meldolesi *et al.* (26). Thus, these secretory granule-like organelles displayed core density and a size of 200–400 nm, and they contained the hormones NPY and GH, but not the lysosomal-associated membrane protein lamp-1. In addition, in the presence of fCgA, the formed granules allowed NPY to be rerouted from a constitutive to a regulated pathway of secretion and were able to release both NPY and GH upon stimulation. These data demonstrate that frog CgA induces the biogenesis of functional DCGs in non-endocrine cells and is capable of orienting a secretory cargo toward a RSP. Although the granin efficiently oriented NPY-Venus from constitutive to regulated pathway of secretion, it seemed less efficient regarding GH, because no difference could be observed for the basal constitutive release of this hormone in the absence or presence of fCgA. This observation suggests that CgA may behave differently depending on cargo proteins. It is possible that other granins like CgB or SgII may act as helpers for cargo-specific proteins. It has been shown that some cell lines such as the somatotroph cell line GH4C1, lacking CgA but containing CgB and SgII (27), are able to sort and release hormones in a regulated manner.

The ability of CgA to form aggregates in the TGN (11) and to interact with other cargo proteins (28, 29) and secretory granule membranes (30) suggests that this protein, probably acting in concert with other granins (14, 28–30), may represent the driving force for granulogenesis (2). It has been shown that CgA interacts with several integral membrane proteins of secretory granules, including the inositol 1,4,5-triphosphate receptor/Ca<sup>2+</sup> channels to control intracellular Ca<sup>2+</sup> release (31–35), or syntaxin 1A and synaptotagmin I, which par-

## Frog CgA Promotes Hormone Sorting

ticipate in the fusion complex formation during exocytic events (36). These protein-protein interactions suggest the possibility of communication between the intragranular matrix proteins and the traffic and fusion machineries. We showed here for the first time that expression of fCgA induces the biogenesis of granules, which exhibit displacements in straight lines, suggesting that the formed vesicles interact with the cytoskeleton in transfected non-endocrine cells. Some of these granules displayed fast movements and disappeared after cell treatment with a  $\text{Ca}^{2+}$  ionophore, whereas others showed restricted movements and were always distinguishable as they remained docked to the plasma membrane after ionophore treatment (videos 5–8 in supplemental data). These two granule populations may correspond to the readily releasable and the reserve pools described in neuroendocrine cells (37). These observations raise the interesting possibility that CgA could be a relevant factor in the mobilization of secretory granules, probably through the induction of interactions between secretory granule proteins and the cytoskeleton elements. Further characterization of the mobility of CgA-induced granules in COS-7 cells will be required to test this hypothesis.

**The Conserved Domains of fCgA Are Instrumental for Granulogenesis**—Our findings show that the conserved terminal regions of fCgA are required for sorting of cargo and granulogenesis. Consistently, it has been shown that the N-terminal region of rat CgA is sufficient to divert a cytosolic protein to the RSP and to induce granulogenesis in PC12 cells (13, 38, 39). In fact, the N-terminal domain of CgA has been proposed to mediate its binding to SgIII, and thereby to cholesterol, because the latter granin protein interacts with the lipid, probably allowing secretory cargo to interact with DCG membranes (28, 30, 39). Such interactions could possibly facilitate budding and formation of ISG at the TGN (2). Our results showed that, in the context of the fCgA protein, deletion of either one of the two conserved N- and C-terminal regions impaired secretory granule formation. This finding indicates that, although the N-terminal peptide taken separately is a sufficient granulogenic determinant (13, 38, 39), other CgA-mediated interactions through its C-terminal conserved regions could play important sorting and granulogenic roles. Consistent with an important role also for the C-terminal domain of CgA in sorting and granulogenesis, earlier studies have shown that this region of CgA is involved in  $\text{Ca}^{2+}$ /pH-dependent homodimerization/homotetramerization (40) allowing the aggregation-mediated sorting of CgA to DCGs (41, 42). In light of these observations, it is evident that both the N- and C-terminal domains of CgA contribute to the sorting and the granulogenic activity of CgA in the RSP in different cell types. The strong conservation of both domains throughout evolution is an argument in favor of their instrumental role in the RSP.

**Targeting of CgA and POMC to the Regulated Secretory Pathway Requires the Conserved Peptides of CgA**—A prominent role of the conserved motifs of CgA in hormone sorting, and secretion was also found in endocrine cells. It is of interest to note that deletion of both the N- and C-terminal domains provoked a marked decrease in the number of secretory granules as well

as in basal release of the resulting protein compared with the forms deleted in either the N or the C terminus. This observation confirms that both conserved terminal regions of CgA are essential for the targeting of the protein to the secretory granules in AtT20 cells and suggests that the forms deleted only in one of the conserved motifs are sorted more efficiently compared with the protein deleted on both sides. This could be accounted for by potential heterotypic dimerization/tetramerization between the singly deleted forms of fCgA and the endogenous CgA, leading to partial sorting of fCgA.

Overexpression of fCgA in AtT20 cells increased POMC levels in the secretory granules, and stimulation of the transfected cells by high potassium triggered the release of the prohormone. This finding suggests that CgA may function as a helper protein for sorting of POMC to the RSP, as it has been previously shown for CgB (43), and is in line with previous observations indicating that CgA levels are highly correlated with POMC storage in pituitary cells (20, 21). Our results also showed that expression of fCgA-truncated forms in AtT20 cells led to retention of POMC in the perinuclear area, despite the expression of the endogenous CgA. This indicates that the N- and/or C-terminal regions play a key role in POMC sorting to DCGs, consistent with previous data showing that POMC interacts with CgA through SgIII and carboxypeptidase E (29). The fCgA deletion mutants are apparently acting as negative-dominants that impair CgA and POMC sorting through the RSP, probably by disrupting the molecular interactions that normally occur between CgA and other secretory helper proteins. Alternatively, the N- and/or C-terminal regions of CgA could be necessary to stabilize POMC post-translationally by up-regulating the expression of the serine protease inhibitor, PN-1, which has been shown to inhibit the degradation of DCG proteins in the TGN (44). Finally, it is also possible that CgA, through its terminal peptides, may inhibit processing enzymes responsible for the conversion of POMC into smaller releasable peptides such as ACTH and  $\beta$ -endorphin, as suggested by previous studies (45) and data reported here showing no variation in ACTH production and release in the presence of fCgA. However, the fact that deletion of the N- and C-terminal peptides of fCgA obliterated the transit of POMC from the TGN to secretory granules indicates that CgA plays a role in sorting of POMC before a putative effect on the processing of the hormone.

In conclusion, the present study took advantage of the structure of a non-mammalian CgA to determine the key role of the granin and its highly conserved peptides in the context of the natural protein, in granulogenesis, and in the sorting of associated hormones in regulated and constitutively secreting cells. The data indicate that CgA is able to orient secretory cargo toward the regulated pathway and that both the N- and C-terminal conserved regions are required to confer to the granin its capacity to form mobile DCGs and to control hormone secretion.

**Acknowledgments**—We thank Drs R. W. Holz and D. Perrais for plasmids. We are also grateful to Huguette Lemonnier for her valuable technical assistance.

## REFERENCES

1. Dannies, P. S. (1999) *Endocr. Rev.* **20**, 3–21
2. Kim, T., Gondré-Lewis, M. C., Arnaoutova, I., and Loh, Y. P. (2006) *Physiology* **21**, 124–133
3. Wang, Y., Thiele, C., and Huttner, W. B. (2000) *Traffic* **1**, 952–962
4. Tooze, S. A., Martens, G. J., and Huttner, W. B. (2001) *Trends Cell Biol.* **11**, 116–122
5. Dikeakos, J. D., and Reudelhuber, T. L. (2007) *J. Cell Biol.* **177**, 191–196
6. Morvan, J., and Tooze, S. A. (2008) *Histochem. Cell Biol.* **129**, 243–252
7. Day, R., and Gorr, S. U. (2003) *Trends Endocrinol. Metab.* **14**, 10–13
8. Taupenot, L., Harper, K. L., and O'Connor, D. T. (2003) *N. Engl. J. Med.* **348**, 1134–1149
9. Montero-Hadjadje, M., Vaingankar, S., Elias, S., Tostivint, H., Mahata, S. K., and Anouar, Y. (2008) *Acta Physiol. (Oxf)* **192**, 309–324
10. Chanat, E., Weiss, U., and Huttner, W. B. (1994) *FEBS Lett.* **351**, 225–230
11. Yoo, S. H. (1996) *J. Biol. Chem.* **271**, 1558–1565
12. Kim, T., Tao-Cheng, J. H., Eiden, L. E., and Loh, Y. P. (2001) *Cell* **106**, 499–509
13. Courel, M., Rodemer, C., Nguyen, S. T., Pance, A., Jackson, A. P., O'Connor, D. T., and Taupenot, L. (2006) *J. Biol. Chem.* **281**, 38038–38051
14. Huh, Y. H., Jeon, S. H., and Yoo, S. H. (2003) *J. Biol. Chem.* **278**, 40581–40589
15. Beuret, N., Stettler, H., Renold, A., Rutishauser, J., and Spiess, M. (2004) *J. Biol. Chem.* **279**, 20242–20249
16. Mahapatra, N. R., O'Connor, D. T., Vaigankar, S. M., Hikim, A. P., Mahata, M., Ray, S., Staite, E., Wu, H., Gu, Y., Dalton, N., Kennedy, B. P., Ziegler, M. G., Ross, J., and Mahata, S. K. (2005) *J. Clin. Invest.* **115**, 1942–1952
17. Kim, T., Zhang, C. F., Sun, Z. Q., Wu, H. L., and Loh, Y. P. (2005) *J. Neurosci.* **25**, 6958–6961
18. Hendy, G. N., Li, T., Girard, M., Feldstein, R. C., Mulay, S., Desjardins, R., Day, R., Karaplis, A. C., Tremblay, M. L., and Canaff, L. (2006) *Mol. Endocrinol.* **20**, 1935–1947
19. Montesinos, M. S., Machado, J. D., Camacho, M., Diaz, J., Morales, Y. G., de la Rosa, D. A., Carmona, E., Castañeyra, A., Viveros, O. H., O'Connor, D. T., Mahata, S. K., and Borges, R. (2008) *J. Neurosci.* **28**, 3350–3358
20. Turquier, V., Vaudry, H., Jégou, S., and Anouar, Y. (1999) *Endocrinology* **140**, 4104–4112
21. Peinado, J. R., Vazquez-Martinez, R., Cruz-Garcia, D., Ruiz-Navarro, A., Anouar, Y., Tonon, M. C., Vaudry, H., Gracia-Navarro, F., Castano, J. P., and Malagon, M. M. (2006) *Endocrinology* **147**, 1408–1418
22. Moore, H. P., and Kelly, R. B. (1985) *J. Cell Biol.* **101**, 1773–1781
23. Montero-Hadjadje, M., Vaudry, H., Turquier, V., Leprince, J., Do Rego, J. L., Yon, L., Gallo-Payet, N., Plouin, P. F., and Anouar, Y. (2002) *Cell Tissue Res.* **310**, 223–236
24. Jégou, S., Tonon, M. C., Leroux, P., Delarue, C., Leboulenger, F., Pelletier, G., Côté, J., Ling, N., and Vaudry, H. (1983) *Gen. Comp. Endocrinol.* **51**, 246–254
25. Malacombe, M., Bader, M. F., and Gasman, S. (2006) *Biochim. Biophys. Acta* **1763**, 1175–1183
26. Meldelesi, J., Chiarelli, E., and Malosio, M. L. (2004) *Trends Cell Biol.* **14**, 13–19
27. Gorr, S. U. (1996) *J. Biol. Chem.* **271**, 3575–3580
28. Hosaka, M., Watanabe, T., Sakai, Y., Uchiyama, Y., and Takeuchi, T. (2002) *Mol. Biol. Cell* **13**, 3388–3399
29. Hosaka, M., Watanabe, T., Sakai, Y., Kato, T., and Takeuchi, T. (2005) *J. Cell Sci.* **118**, 4785–4795
30. Hosaka, M., Suda, M., Sakai, Y., Izumi, T., Watanabe, T., and Takeuchi, T. (2004) *J. Biol. Chem.* **279**, 3627–3634
31. Yoo, S. H. (1994) *J. Biol. Chem.* **269**, 12001–12006
32. Yoo, S. H., and Jeon, C. J. (2000) *J. Biol. Chem.* **275**, 15067–15073
33. Thrower, E. C., Park, H. Y., So, S. H., Yoo, S. H., and Ehrlich, B. E. (2002) *J. Biol. Chem.* **277**, 15801–15806
34. Thrower, E. C., Choe, C. U., So, S. H., Jeon, S. H., Ehrlich, B. E., and Yoo, S. H. (2003) *J. Biol. Chem.* **278**, 49699–49706
35. Choe, C. U., Harrison, K. D., Grant, W., and Ehrlich, B. E. (2004) *J. Biol. Chem.* **279**, 35551–35556
36. Yoo, S. H., You, S. H., and Huh, Y. H. (2005) *FEBS Lett.* **579**, 222–228
37. Becherer, U., and Rettig, J. (2006) *Cell Tissue Res.* **326**, 393–407
38. Taupenot, L., Harper, K. L., Mahapatra, N. R., Parmer, R. J., Mahata, S. K., and O'Connor, D. T. (2002) *J. Cell Sci.* **115**, 4827–4841
39. Han, L., Suda, M., Tsuzuki, K., Wang, R., Ohe, Y., Hirai, H., Watanabe, T., Takeuchi, T., and Hosaka, M. (2008) *Mol. Endocrinol.* **22**, 1935–1949
40. Yoo, S. H., and Lewis, M. S. (1993) *Biochemistry* **32**, 8816–8822
41. Chanat, E., and Huttner, W. B. (1991) *J. Cell Biol.* **115**, 1505–1519
42. Cowley, D. J., Moore, Y. R., Darling, D. S., Joyce, P. B., and Gorr, S. U. (2000) *J. Biol. Chem.* **275**, 7743–7748
43. Natori, S., and Huttner, W. B. (1996) *Proc. Natl. Acad. Sci. U. S. A.* **93**, 4431–4436
44. Kim, T., and Loh, Y. P. (2006) *Mol. Biol. Cell* **17**, 789–798
45. Seidah, N. G., Hendy, G. N., Hamelin, J., Paquin, J., Lazare, C., Metters, K. M., Rossier, J., and Chrétien, M. (1987) *FEBS Lett.* **211**, 144–150